

Pediatric Lens Dose Coefficients for Photons and Electrons: Dosimetric Impact of Detailed Eye Models for ICRP Paediatric Mesh-type Reference Computational Phantoms

Haegin Han^a, Yeon Soo Yeom^b, Chansoo Choi^a, Bangho Shin^a, Sungho Moon^a, Sangseok Ha^a, Thang Tat Nguyen^c,
Chan Hyeong Kim^{a*}

^a Department of Nuclear Engineering, Hanyang University, 222 Wangsimni-ro, Seongdong-gu, Seoul 04763, Korea

^b National Cancer Institute, National Institute of Health, 9609 Medical Center Drive, Bethesda, MD 20850, USA

^c School of Nuclear Engineering and Environmental Physics, Hanoi University of Science and Technology, 1 Dai Co Viet Road, Hanoi, Vietnam

* Corresponding author: chkim@hanyang.ac.kr

1. Introduction

The International Commission on Radiological Protection (ICRP) recently reduced the annual equivalent dose limit of eye lens from 150 mSv to 20 mSv, for occupational exposure in planned exposure situations [1], highlighting the importance of accurate estimation of dose to the lens of the eye.

For the accurate lens dose calculations, in Publication 116 [2], the ICRP used the detailed eye model developed by Behrens et al. [3] for the calculation of lens dose coefficients (DCs) for weakly penetrating radiations, which cannot be accurately calculated with the voxel-type reference phantoms [4] due to their limited voxel resolutions ($2.137 \times 2.137 \times 8 \text{ mm}^3$ for male and $1.775 \times 1.775 \times 4.84 \text{ mm}^3$ for female). The Behrens' detailed eye model [3] was recently incorporated into the new ICRP mesh-type reference computational phantoms (MRCPs) for adult male and female [5,6].

The detailed eye model of Behrens et al. [3], however, was developed based on ocular dimensions for adults, and thus is inappropriate to be used for pediatric lens dose calculations. Recently, Vejdani-Noghreiyani and Ebrahimi-Khankook [7] developed pediatric detailed eye models for 5-, 10-, and 15-year olds, based on the same data to those used for the construction of the adult eye model [8]. However, these data are mostly for adult ages and are lack of the data measured from pediatric eyes. In addition, these eye models do not include those for younger ages (i.e., the newborn and 1-year old). Therefore, as presented in the previous KNS meeting [9], we developed a full set of pediatric detailed eye models for newborn 1-, 5-, 10-, and 15-year olds by determining nine ocular parameters for each age based on various scientific literatures that performed *in vivo* measurement of pediatric eyes.

As the follow-up of Han et al. [9], in the present study, the pediatric eye models were finalized by slightly modifying a few ocular parameters and by deciding densities and elemental compositions of the subregions of the eye models. The constructed eye models were then incorporated into the pediatric MRCPs. The pediatric MRCPs with detailed eye models were then used to calculate the lens DCs for the external exposures to photons and electrons. Finally, the calculated pediatric lens DCs were compared with those

calculated with the eye models of adult MRCPs [10] and Vejdani-Noghreiyani and Ebrahimi-Khankook [7].

2. Material and Methods

2.1 Finalization of Pediatric Detailed Eye Models

In the final stage of development, some ocular dimensions of the previously developed pediatric eye models [9] were slightly changed. Among the nine ocular parameters (i.e., anterior chamber depth along the optical axis (ACD), lens thickness along the optical axis (LT), radius of curvature of the anterior surface of the lens (RAL), radius of curvature of the posterior surface of the lens (RPL), radius of curvature of the anterior surface of the cornea (RAC), corneal thickness along the optical axis (CT), corneal diameter (CD), equatorial diameter of the lens (ED), radius of curvature of the anterior surface of the sclera (RAS)), changes were made only on ED and RAS.

For the determination of the ED values, the previously used references, which measured eye lens *in vitro*, were replaced by 93 data points pooled from several studies [11-16] that were performed *in vivo* measurements. The pooled data were fitted to natural logarithmic, logarithmic, and double log functions, and age-dependent ED values were determined by averaging those derived from these three fitting functions. In addition, RAS values were slightly modified to match the blood-inclusive eye masses derived from regional blood fraction and reference eye mass given in Wayson et al. [17] and ICRP Publication 89 [18], respectively.

Among the five subregions defined in the detailed eye models (i.e., sensitive/insensitive lens, aqueous humour, vitreous humour, and cornea), the density of the lens regions, which has strong age dependence [18], was decided for each age by using the fitting function derived from 127 data provided by Prof. Augusteyn. The densities of the other regions and elemental compositions of the all regions were derived from those used in Behrens et al. [3], by assuming the homogenous blood distribution in eye regions except for lens [18].

2.2 Incorporation into Pediatric MRCPs

The pediatric detailed eye models, which were constructed in mathematical models, were first converted into the mesh format and incorporated into pediatric MRCPs, following the approach used in Nguyen et al. [6].

2.3 Calculation of Lens Dose Coefficients

Lens DCs were calculated for external photons and electrons in the energy range of 0.01-10,000 MeV in irradiation geometries considered in ICRP Publication 116 [2] (i.e., AP, PA, RLAT, LLAT, ROT, and ISO for photons; AP, PA, and ISO for electrons). To save the computational time, for the photon and electron energies lower than 10 MeV, the radiation sources were defined to cover only the head of the phantoms, under the assumption that the contribution of the secondary radiations from the other body parts are negligible [6].

Monte Carlo dose calculations were performed by implementing the tetrahedralized pediatric MRCPs into Geant4 (version 10.06.p02). The physics library of *G4EMLivermorePhysics* was used and a secondary cut range value was set as 1 μm , considering the micrometer-scale structure of the detailed eye models. The number of primary particles was set to keep the relative errors for lens DCs below 5%.

3. Results

3.1 Pediatric Eye Models Incorporated into MRCPs

Table 1. Nine ocular parameters determined for pediatric detailed eye models (unit: mm).

	newborn	1-year	5-years	10-years	15-years
ACD	1.83	2.75	2.90	3.16	3.21
LT	3.96	3.66	3.61	3.41	3.44
RAL	6.33	9.23	10.51	11.45	11.72
RPL	4.48	5.27	6.05	6.24	6.55
RAC	7.11	7.82	7.72	7.72	7.72
CT	0.55	0.55	0.56	0.57	0.57
CD	9.66	2.75	11.80	11.80	11.80
ED	5.85	3.66	8.03	8.57	8.89
RAS	9.08	9.45	10.96	11.30	11.63



Fig. 1. Pediatric detailed lens model incorporated into the newborn male MRCP.

Table 1 lists the nine ocular parameters finalized for the pediatric detailed eye models for the newborn and 1-, 5-, 10-, 15-year olds and Fig. 1 shows the newborn eye model incorporated into the newborn male MRCP, as an example. It can be seen that the eye models were well installed in the center of the orbital center of the cranium. Note that the densities and elemental compositions of the subregions of the eye models were not given here due to the lack of the space, but will be presented during presentation.

3.2 Pediatric Lens Dose Coefficients

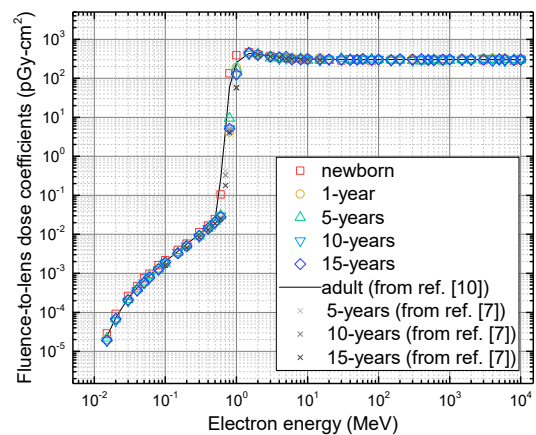


Fig. 2. Lens DCs calculated for electrons in AP direction, compared with those calculated with the eye models of adult MRCPs (solid line) and Vejdani-Noghreiyani and Ebrahimi-Khankook [7] (X marks).

Fig. 2 shows the lens DCs calculated for electrons in the AP geometry, for an example, compared with those calculated with the eye models of adult MRCPs and Vejdani-Noghreiyani and Ebrahimi-Khankook [7]. Note that these two external lens DC data were taken from reference literatures [7,10], and the former data [7] provides DCs only for the energy range of 0.1-10 MeV.

When the lens DCs of the present study were compared with those calculated with adult MRCPs, the largest differences were found at the energies in the transition region (i.e., 0.6-1 MeV), in which the lens DCs of the newborn were larger than those of the adult by up to ~ 2 times, while those of the other pediatric ages were, on average, ~ 10 times smaller. This tendency is explained by the fact that the depth of the pediatric lens, especially the smallest depth which is the lens depth at its peripheral region, is smaller than that of the adult in the newborn eye model and larger in the other pediatric ages. Note that the depth of the lens significantly affects lens DCs in this energy range, because the transition region is where the primary electrons start to reach the lens and directly deposit their energy to the lens. Outside the transition region, the differences in DCs between the pediatric and adult MRCPs were much smaller, i.e., generally less than 20%.

Similarly, in the transition region, the lens DCs of the present study were significantly larger than those of Vejdani-Noghreiyani and Ebrahimi-Khankook [7], showing the differences up to the factor of ~3 for 5-year old at 1 MeV. This is due to the fact that while the lens DCs of MRCPs were calculated in radiosensitive region of the lens, those of the Vejdani-Noghreiyani and Ebrahimi-Khankook [7] were calculated in the whole lens. That is, for the radiations that yield high dose gradient in lens region, the sensitive region of the lens distributed in the in front of the lens can receive much higher doses than the doses averaged over the whole lens. Again, for the other energy regions, the differences were generally less than 15%.

4. Conclusions

In the present study, the pediatric detailed eye models, presented in the previous KNS meeting, were finalized and incorporated into the pediatric MRCPs. The pediatric MRCPs with the detailed eye models were then used to calculate the lens DCs for external photons and electrons. In this paper, as an example, the lens DCs for electrons in the AP geometry were shown and compared with those calculated the adult MRCPs and pediatric detailed eye models of Vejdani-Noghreiyani and Ebrahimi-Khankook [7]. For both comparison targets, the largest differences were found in transition region (0.6-1 MeV), which was mainly due to the lens depth and definition of radiosensitive region of the lens, respectively. The pediatric lens DCs calculated in the present study, as well as pediatric eye models, are expected to be a useful tool in various applications that requires accurate lens dose assessment for pediatric ages.

REFERENCES

- [1] ICRP, ICRP Statement on Tissue Reactions / Early and Late Effects of Radiation in Normal Tissues and Organs – Threshold Doses for Tissue Reactions in a Radiation Protection Context. ICRP Publication 118. Ann. ICRP 41(1/2), 2012.
- [2] ICRP, Conversion coefficients for radiological protection quantities for external radiation exposures, ICRP Publication 116, Ann. ICRP 40 (2-5), 2010.
- [3] R. Behrens, G. Dietze, and M. Zankl, Dose conversion coefficients for electron exposure of the human eye lens. *Physics in medicine and biology* 54.13: pp. 4069, 2009.
- [4] ICRP, Adult reference computational phantoms, ICRP Publication 110, Ann. ICRP 39 (2), 2009.
- [5] ICRP, Adult Mesh-type Reference Computational Phantoms, ICRP Publication 145, Ann. ICRP (in press)
- [6] T. T. Nguyen, et al., Incorporation of detailed eye model into polygon-mesh versions of ICRP-110 reference phantoms, *Physics in medicine and biology* 60.22: pp. 8695-8707, 2015.
- [7] A. Vejdani-Noghreiyani and A. Ebrahimi-Khankook, An age-dependent series of eye models for radiation dosimetry. *Physics in medicine and biology* 64.13: 135004, 2019.
- [8] M. W. Charles and N. Brown, Dimensions of the human eye relevant to radiation protection (dosimetry). *Physics in medicine and biology* 20.2: pp. 202, 1975.
- [9] H. Han, et al., Development of Detailed Eye Models for Pediatric Phantoms. *Transactions of Korean Nuclear Society Autumn Meeting*, 2017.
- [10] Y. S. Yeom, et al., Dose coefficients of mesh-type ICRP reference computational phantoms for idealized external exposures of photons and electrons. *Nuclear Engineering and Technology* 51.3: 843-852, 2019.
- [11] D. A. Atchison, et al., Age-related changes in optical and biometric characteristics of emmetropic eyes. *Journal of vision* 8.4: 29-29, 2008.
- [12] G. Dilmen, et al., Growth of the fetal lens and orbit. *International journal of gynecology and obstetrics* 76.3: 267-271, 2002.
- [13] I. Goldstein et al., Growth of the fetal orbit and lens in normal pregnancies. *Ultrasound in Obstetrics and Gynecology: The Official Journal of the International Society of Ultrasound in Obstetrics and Gynecology* 12.3: 175-179, 1998.
- [14] K. Ishii, et al., Relationship between changes in crystalline lens shape and axial elongation in young children. *Investigative ophthalmology and visual science* 54.1: 771-777, 2013.
- [15] L. B. Paquette, et al., In utero eye development documented by fetal MR imaging. *American journal of neuroradiology* 30.9: 1787-1791, 2009.
- [16] K. Sukonpan and V. Phupong, A biometric study of the fetal orbit and lens in normal pregnancies. *Journal of clinical ultrasound* 37.2: 69-74, 2009.
- [17] M. B. Wayson, et al., Suggested reference values for regional blood volumes in children and adolescents. *Physics in Medicine and Biology* 63.15: 155022, 2018.
- [18] ICRP, Basic Anatomical and Physiological Data for Use in Radiological Protection Reference Values. ICRP Publication 89. Ann. ICRP 32 (3-4), 2002.